$Ca_4Cu_5O_{10}$: Copper oxide chains highly occupied by Zhang-Rice singlets

A. Hayashi*
Department of Chemistry and Princeton Materials Institute, Princeton University, Princeton, New Jersey 08540

B. Batlogg
Bell Laboratories, Lucent Technologies, Murray Hill, New Jersey 07974

R. J. Cava
Department of Chemistry and Princeton Materials Institute, Princeton University, Princeton, New Jersey 08540
(Received 5 February 1998)

The crystal structure of $Ca_{2+x}Y_{2-x}Cu_5O_{10}$ consists solely of one-dimensional copper-oxygen chains made from CuO_4 squares sharing edges. Over the range of x between 0 and 2, here synthesized using high-pressure oxygen annealing, formal copper valences between 2 and 2.4 can be obtained. All the members of the series are electrically insulating. Magnetization measurements show long-range antiferromagnetic ordering near $x=0$, with decreasing T_N on increasing x, and the appearance of a new kind of short-range-ordered state for x greater than 1.5. The high hole concentration regime represents the first observation of the magnetic and transport properties of a mixture of Zhang-Rice singlets and magnetic copper on one-dimensional chains without the complication of additional copper-oxygen units, and may be an excellent model system for studying their spin and charge dynamics as a key to understanding the behavior of CuO_2 planes in copper oxide superconductors. [S0163-1829(98)00329-4]

INTRODUCTION

Detailed understanding of the charge and spin dynamics in the electronically doped CuO_2 planes central to the occurrence of superconductivity in copper oxides remains elusive. Recent exploration of spin-ladder compounds such as $SrCu_2O_3$ and $(Sr,Ca)_{14}Cu_{24}O_{41}$ has forged a link between experimental studies and first-principles calculations of the expected properties of spin systems related to the CuO_2 planes,[1] but for the pure ladder compounds, electronic doping has not been possible.[2–5] In the more complex compound, $(Sr,Ca)_{14}Cu_{24}O_{41}$, doping is possible, even leading to superconductivity under some conditions,[6] but the distribution of doped holes between the CuO_2 chains and Cu_2O_3 ladders is complicated due to competition between the two potential hole acceptors.[7–9] Here we present the results of studies of the $Ca_{2+x}Y_{2-x}Cu_5O_{10}$ series of compounds, which have only one electronically active component—infinite chains of edge-linked CuO_4 squares. To our knowledge, it is the first compound to be reported in which such one-dimensional (1D) chains can be doped with holes without additional electronic complications. In contrast to the chains of corner-linked squares common in high-T_c copper oxides, where the exchange interaction (J) between Cu^{2+} ions is large due to 180° Cu-O-Cu superexchange, J for edge-shared squares is greatly weakened due to the presence of 90° superexchange. The lower exchange coupling allows the high-temperature magnetic properties of the system to be probed, and reveals that the magnetic ground state crosses over from a Néel state to a new type of short-range-ordered state as a function of hole concentration. The change in the magnetic superexchange in this high hole concentration regime is attributed to the presence of a very large number of Zhang-Rice singlets,[10] widely believed to be an important part of the understanding of the CuO_2 planes in cuprate.

The compound $Ca_4Cu_5O_{10}$ was identified[11] as a low-temperature phase, stable below about 750 °C, and later shown[12] to be stabilized at higher temperature by applying oxygen pressures of 10 bars. Recently, the Sr analog of this compound was prepared at high pressure.[13] Partial Y substitution for Ca was reported,[14,15] in the solid solution $Ca_{2+x}Y_{2-x}Cu_5O_{10}$, with $0<x<0.8$ in air at 1000 °C. The structure for these phases is closely related to that of $NaCuO_2$,[16] which contains edge-shared CuO_4 squares forming infinite CuO_2 chains, with Na in distorted octahedral coordination between chains. In contrast to $NaCuO_2$, where all available octahedral sites are occupied with Na, the Ca and Y containing phases have 20% fewer large cations per copper, leading to a complex, sometimes incommensurate relationship between the Ca/Y chain repeat distance and the Cu chain repeat distance.[15] Figure 1 shows a schematic structure for $Ca_4Cu_5O_{10}$, where five CuO_4, squares share edges along the chain parallel to a in the same distance that four Ca repeat between the chains. The chains are stacked in a staggered fashion above one another with no intervening oxygen, and there is also no intervening oxygen between chains in the same layer. The separation between the Cu in the chain stacking direction is 3.4 Å, very close to that observed in the corner-shared chain compounds $Sr_2CuO_3$and Ca_2CuO_3.

Here we report the successful synthesis of the solid solution $Ca_{2+x}Y_{2-x}Cu_5O_{10}$ ($0<x<2$) by high-pressure oxygen annealing. The solid solution spans the range of formal copper valences from $Cu^{2+}$to $Cu^{2.4+}$, allowing the observation of the magnetic and electrical properties over a wide range of hole concentration, 0 to 0.4–0.5 holes per Cu. One CuO_4 plaquette is rendered nonmagnetic for each doped hole.[17] The effective interaction between magnetic sites becomes more antiferromagnetic with hole doping and the ground state crosses over from a Néel state to a short-range ordered state. Although the compounds become somewhat conduc-

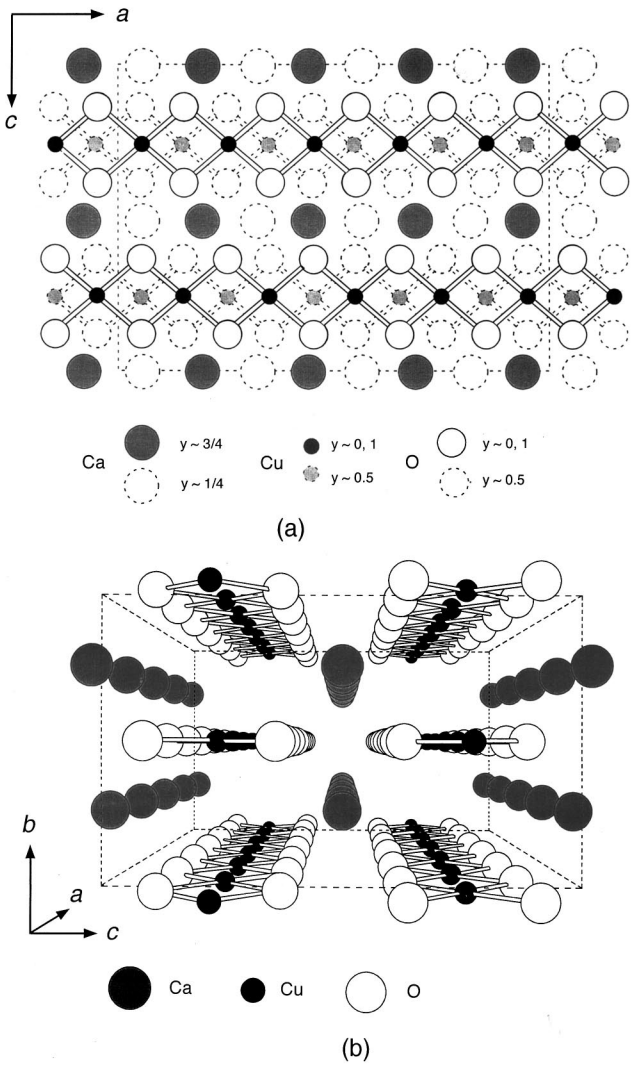

FIG. 1. Schematic structure for $Ca_4Cu_5O_{10}$. (a) Projection onto the *ac* plane, (b) perspective view along the *a* axis. Dotted lines indicate the unit cell.

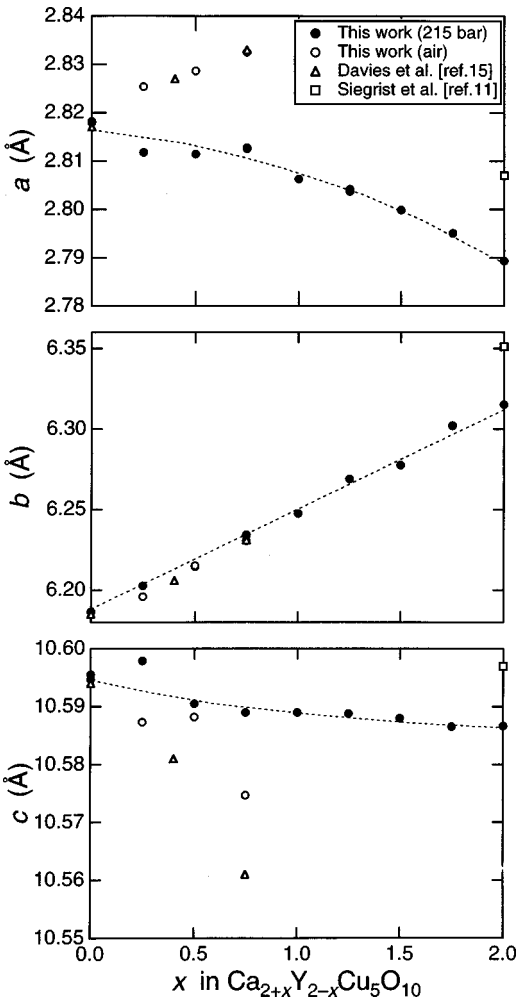

FIG. 2. Composition dependence of the subcell lattice parameters for the solid solution $Ca_{2+x}Y_{2-x}Cu_5O_{10-\delta}$.

tive with the introduction of holes, the holes are apparently localized, with the materials remaining insulating, in dc measurements, over the whole series.

SYNTHESIS AND STRUCTURE

Polycrystalline samples were prepared from high-purity Y_2O_3, $CaCO_3$, and CuO by solid-state reaction. Starting materials were mixed and heated in air at 900 °C for 12 h in Al_2O_3 crucibles. The products were then ground, pelletized, and heated at 1000 °C in air for 120 h with several intermediate grindings. High-pressure oxygen annealing was performed in a commercially available high-pressure furnace (Morris Research). Pressed samples on gold foil were heated at 1000 °C under oxygen pressure of 215 ± 5 bars for 48 h. After being ground and pelletized, the treatment was repeated to insure complete reaction. Phase identification was carried out by powder x-ray diffraction with Cu $K\alpha$ radiation. Lattice parameters were calculated by the least-squares method. The oxygen content on selected samples was determined by thermogravimetic analysis (TGA) under forming gas (5% H_2/N_2). The magnetization was measured using a superconducting quantum interference device (SQUID) magnetometer in the temperature range from 2 to 400 K. The electrical resistivity was measured by a standard dc four-probe method.

In air at 1000 °C, a solid solution of $Ca_{2+x}Y_{2-x}Cu_5O_{10}$ was formed in the composition range $0.03<x<1.0$, roughly consistent with the previous results obtained under similar experimental conditions.[14] Using the high-pressure oxygen annealing process described above, the upper limit of the solid solution could be extended to $x=2.0$, $Ca_4Cu_5O_{10}$. The powder x-ray diffraction pattern for all samples could be indexed on the basis of an orthorhombic Fmmm subcell; $a\sim2.8$ Å, $b\sim6.25$ Å, and $c\sim10.6$ Å, which averages out the incommensurability of the supercell, but characterizes the essential structural features relevant to the present discussion. Figure 2 shows composition dependence of the subcell lattice parameters for samples prepared in this study, together with the previous results. Reflecting the difference in ionic radii for Ca^{2+} (1.0 Å) and Y^{3+} (0.9 Å), the variation of the subcell parameters in the solid solution range is small; 1, 2, and 0.1 % for the *a*, *b*, and *c* axes, respectively. The larger Ca radius influences the structure by increasing the *b* axis, and the introduction of holes effectively compresses the CuO_2 chains (along *a*), decreasing the Cu-O-Cu bond angle.

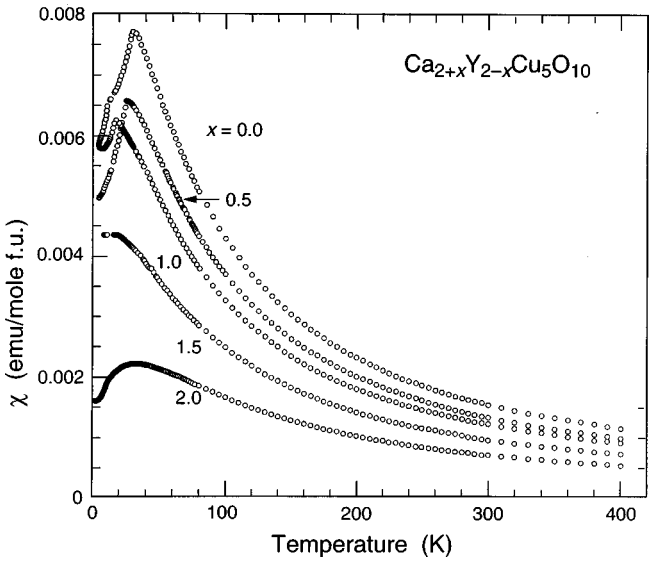

FIG. 3. Temperature dependence of the magnetic susceptibility for several samples in the $Ca_{2+x}Y_{2-x}Cu_5O_{10}$ solid solution.

The composition dependence is different for samples prepared in air and those prepared under high-pressure oxygen, except for the *b* axis. Preliminary TGA studies show this is due to a small difference in oxygen content for $x<1$ for samples prepared in different ambient atmospheres. For the measurements of the magnetic and electrical properties described below, we employed a series of samples prepared under high-pressure oxygen with the exception of $x=0$, which could be synthesized in considerably higher purity in air. The essential features of the magnetic properties were insensitive to the small changes in hole concentration induced by the oxygen stoichiometry differences obtained in different synthetic conditions. The study of detailed phase relations and oxygen stoichiometry as a function of oxygen pressure and temperature is in progress, and will be reported elsewhere.

MAGNETIC AND ELECTRICAL PROPERTIES

Holes introduced into a CuO_4 plaquette such as those which share edges to form the chains in the current compounds occupy mainly the oxygen *p* orbitals which are hybridized with the Cu *d* states. The spin of the hole on the oxygen square couples antiferromagnetically to that of the Cu, canceling its spin, thus rendering the CuO_4 unit nonmagnetic, as pointed out by Zhang and Rice (a Zhang-Rice singlet).[10] Figure 3 shows the temperature dependence of the magnetic susceptibility per Cu for several members of the series from the undoped case ($Y_2Ca_2Cu_5O_{10}$) to the maximally doped case ($Ca_4Cu_5O_{10}$). At first glance, the overall shape of $\chi(T)$ is seen to be that of spins coupled by a moderately weak interaction strength, i.e., $|J|/k_B<100$ K. For the undoped compound $Y_2Ca_2Cu_5O_{10}$, the high-temperature part ($T>150$ K) is well described by a Curie-Weiss law with a net effective *antiferromagnetic* coupling θ of -4.5 ± 0.7 K and a powder averaged *g* factor of 2.25 ± 0.03. In $La_6Ca_8Cu_{24}O_{41}$, which has similar Cu-O chains, the net interaction is *ferromagnetic*,[9] $\theta=10$ K, likely due to the fact that the Cu-O-Cu bond angle in the 14:24:41 phase is closer to 90° than in the present compound. Ferromagnetically coupled edge-shared chains are also observed in Li_2CuO_2.[18] For the composition range $0<x<1$, the magnetic susceptibility curves show a well-defined cusp at low temperatures, indicative of long-range antiferromagnetic order. (For the sample with $x=0$, a small anomaly was observed as a shoulder near 10 K due to the presence of a small amount (≈1%) of highly magnetic $Y_2Cu_2O_5$. With increasing *x* in $Ca_{2+x}Y_{2-x}Cu_5O_{10}$, the data show T_N to decrease and then disappear near $x=1$ due to the introduction of holes: $T_N=28$, 24, and 16 K for $x=0$, 0.5, and 1, respectively. Above $x=1.5$, broad maxima appear in the susceptibility curves (T_{max}). The value of T_{max} increases with increasing *x*, reaching 32 ± 1 K for $Ca_4Cu_5O_{10}$ ($x=2.0$). This feature in the susceptibility represents the magnetic response of the chain system with a high concentration of Zhang-Rice singlets, 4–5 of every ten CuO_4 plaquettes. The tentative magnetic phase diagram based on these data is shown in Fig. 4(a).

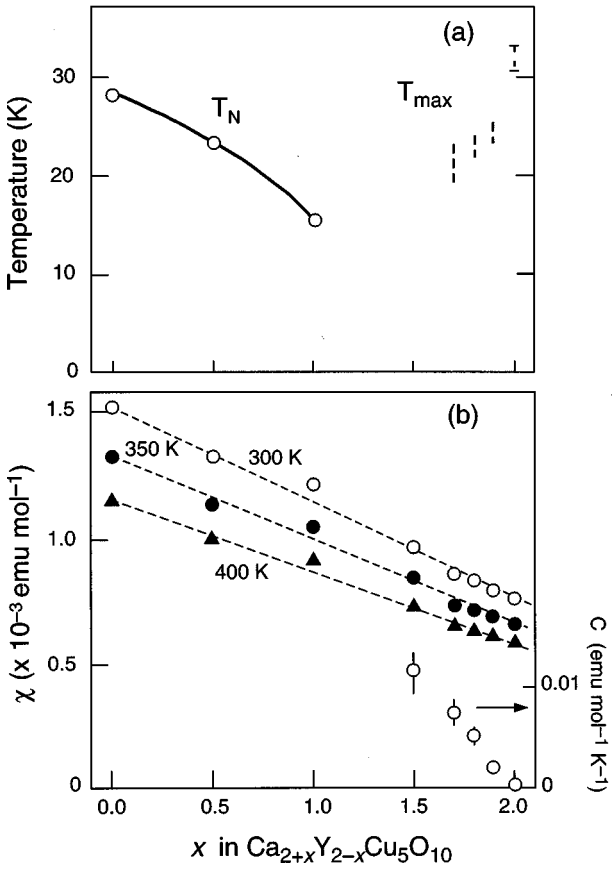

FIG. 4. (a) Tentative magnetic phase diagram for $Ca_{2+x}Y_{2-x}Cu_5O_{10}$, (b) composition dependence of the magnetic susceptibility per Cu for several high temperatures, showing the scaling of the chemical and electronic doping and Curie-like contribution at low temperature.

Due to the weak magnetic interactions in these compounds, the magnetic susceptibility at high temperatures is a measure of the concentration of magnetic copper, and can be employed to determine the effectiveness of the chemical doping in the introduction of holes and the cancellation of Cu spins on the chains. The high-temperature susceptibilities decrease in a precise and systematic manner with increasing Ca content, shown in Fig. 4(b), for $T=300$, 350, and 400 K.

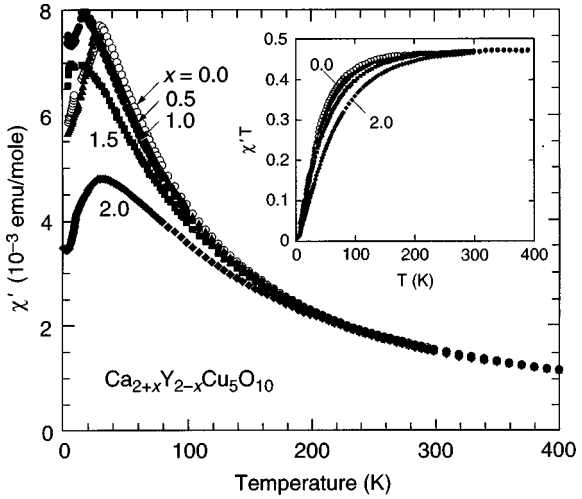

FIG. 5. The temperature dependence of the magnetic susceptibility per magnetic Cu, $\chi'(T)$, for $Ca_{2+x}Y_{2-x}Cu_5O_{10}$. Inset, the $\chi'(T)\times T$ product as a function of temperature and composition.

The values for $Ca_4Cu_5O_{10}$ are, within an experimental error of a few percent, 50% of those found for $Y_2Ca_2Cu_5O_{10}$. Thus the high-temperature susceptibilities are slightly lower than what is expected for a straightforward introduction of exactly one nonmagnetic copper per doped Ca and a constant oxygen content across the series of exactly ten oxygen per formula unit. A small oxygen nonstoichiometry, $\approx$2–3 %, would account for the somewhat increased effectiveness in spin cancellation observed upon introduction of Ca. Also shown, in the lower right corner of Fig. 4(b) is the magnitude of a small Curie-like contribution of $\chi(T)$ observed at the lowest temperatures for $x>1.5$ but not for $x<1.5$ (i.e., only in the high hole concentration regime). This ''impurity'' contribution corresponds to 2.7 ± 0.4% of free Cu moments for $x=1.5$ and decreases linearly as a function of Ca concentration, to zero for $Ca_4Cu_5O_{10}$. These free spins are not likely to be due to the presence of chemical impurities, which were not detected in the x-ray-diffraction experiments, but rather are more likely due to special sites on the Cu-O chains which are neither compensated by a hole nor participating in the short-range antiferromagnetic order. Similar magnetic defect sites were also observed in the related compound $(Sr,Ca)_{14}Cu_{24}O_{41}$.[9]

Given the excellent scaling [Fig. 4(b)] between the number of chemically doped holes and the number of magnetic Cu, the $\chi(T)$data can be replotted as susceptibility per magnetic copper, χ' to separate the effects of dilution from the effects of changing interactions. This is presented in Fig. 5. Above approximately 250 K the data are independent of Ca content, as described above, while at lower temperatures they differ markedly. There is very little difference between the data for samples with x between 0 and 1 over the whole temperature range, except for a decrease in T_N as would be expected for a simple dilution of spins. On approaching $Ca_4Cu_5O_{10}$, however, the susceptibility per magnetic copper decreases significantly and the sharp peak characteristic of long-range order gives way to a broad, rounded maximum at 32 K.

The changeover in response of the magnetic Cu with hole concentration is further illustrated in the inset, for which the $\chi'(T)\times T$ product per magnetic Cu is shown as a function of temperature for all compositions. For temperature-independent spins, and temperatures far above the effective interaction temperature θ, this product will be temperature independent. This is seen to be true for the present case, with the additional fact that the scaling of the magnetism through the number of chemically doped holes is a good description of the system. At high temperatures, all compositions approach a constant $\chi'\times T$ of 0.472, corresponding to a powder averaged g factor of 2.25 ± 0.03. There is very little difference in $\chi'\times T$ for different hole doping levels in the Néel state regime, for x between 0 and 1, indicating essentially unchanged interactions among the magnetic Cu. At low temperatures for $Y_{0.5}Ca_{3.5}Cu_5O_{10}$ and $Ca_4Cu_5O_{10}$, however, $\chi'\times T$ falls significantly below the other curves. This indicates an increase in the effective antiferromagnetic interaction among the magnetic Cu in the high hole concentration regime.

At low-doped Ca concentrations, the sharp drop in $\chi(T)$ indicates the development of long-range antiferromagnetic order, which is rapidly lost beyond a doping level of 0.2 holes per Cu. For a purely one- or two-dimensional (2D) $S=1/2$ Heisenberg magnet, the Néel state is not expected, and thus reflects the presence of residual magnetic interactions, which arise from the coupling to adjacent chains. It is reasonable to expect that the coupling between chains in the present case is similar in magnitude to that observed in other chain compounds such as Ca_2CuO_3 and Sr_2CuO_3, where the interchain coupling is on the order of 10 K. In those compounds, with corner-shared CuO plaquettes, and thus approximately 180° Cu-O-Cu bonds, the intrachain coupling is very large, 1000–2000 K,[19–22] compared to the interchain coupling: in edge-shared plaquette system such as the present one, they can be of the same magnitude.

When holes are introduced into the chains of $Ca_{2+x}Y_{2-x}Cu_5O_{10}$ by Ca doping beyond $x=1$, the magnetic interactions are drastically altered: $\chi(T)$ becomes characteristic of that of short-range order in low-dimensional magnetic systems. At our maximum doping level, nearly one of every two CuO_4 plaquettes is occupied by a nonmagnetic Zhang-Rice singlet. These singlets, which involve holes on the oxygen p orbitals therefore are found to greatly influence the superexchange pathways between the remaining magnetic CuO_4 plaquettes. As is clearly seen by considering the data presented in Fig. 5, the effect is different from what is found for a simple dilution of spins, such as is observed in the low hole doping regime. The detailed functional form of $\chi(T)$ for $Ca_4Cu_5O_{10}$, however, is not that commonly found to describe either 1D chain or 2D plane magnetic systems with only nearest-neighbor Heisenberg interactions. Attempts were made, without success, to fit the observed $\chi(T)$ for $Ca_4Cu_5O_{10}$ to magnetic models such as those for alternate J linear chains, J_1-J_2 linear chains, and weakly interacting uniform chains. These models could not simultaneously describe the temperature of the maximum and the relative broadness of the peak. To our knowledge there has been no study of the expected behavior of such a dense mixture of magnetic spin of Cu and nonmagnetic singlets distributed on chains. It is not known at this time whether there is any structural ordering—either long-range or short-range—of the magnetic singlets. Depending on how the singlets are or-

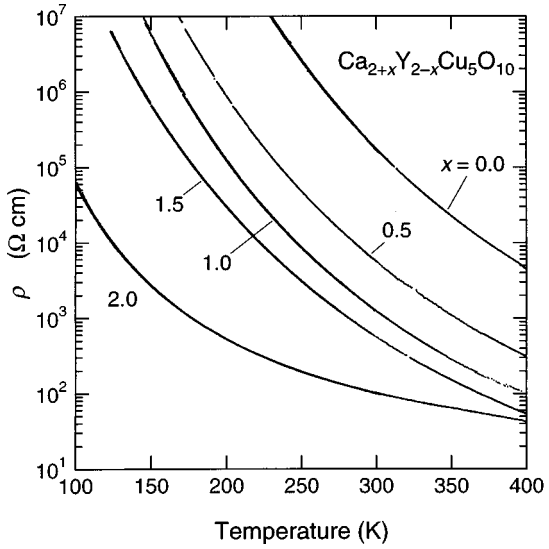

FIG. 6. The temperature dependence of the electrical resistivity for polycrystalline samples of $Ca_{2+x}Y_{2-x}Cu_5O_{10}$.

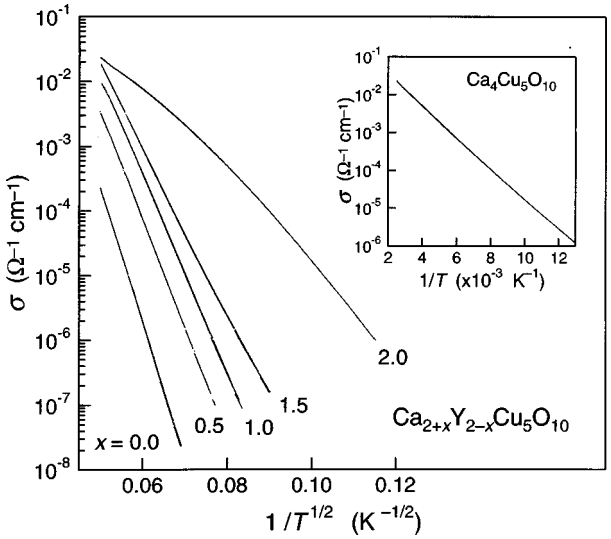

FIG. 7. Log plot of the electrical conductivity σ vs $1/T^{1/2}$ for polycrystalline samples of $Ca_{2+x}Y_{2-x}Cu_5O_{10}$. Shown also, for $Ca_4Cu_5O_{10}$ is a plot of $\ln\sigma$ vs $1/T$.

dered or disordered on the chains or between chains, the resulting interchain coupling may be comparable or larger than the intrachain coupling. For $(Sr,Ca)_{14}Cu_{24}O_{41}$, the magnetic Cu mixed with Zhang-Rice singlets on the chain component of the structure have been shown to order into spin-singlet dimers at certain lattice sizes and hole concentrations.[9] In the present case, in which there can be no mediating electronic interactions due to the presence of other Cu-O components, such as ladders, the behavior is different—no dimerization is observed.

The temperature dependence of the dc resistivities of polycrystalline samples are shown in Fig. 6. The overall resistivities are high, and increase with decreasing temperature. Even for $Ca_4Cu_5O_{10}$, which has a hole doping of approximately 0.5 holes per Cu, the resistivity of $\approx 40\ \Omega$ cm is about five orders of magnitude larger than that of metallic cuprates at similar doping levels. The data suggest that the functional form of $\sigma(T)$ is dependent on hole concentration, changing in character at the same doping level where the magnetic susceptibility changes. This is better illustrated in Fig. 7, which shows the variation of $\log_{10}\sigma$ with $1/T^{1/2}$. Power-law plots of the type $\log_{10}\sigma$ vs $1/T^{1/n}$ for $n \neq 2$ show curvature for all compositions. For hole doping levels between 0.0 and 0.2 per Cu, where the magnetic interactions are well described in a conventional picture, $\sigma(T)$ follows the behavior $\sigma(T) \propto \exp(T^{-1/2})$ very closely, characteristic of variable range hopping in a 1D system. Because the resistivity involves real charge transfer along the Cu-O chains, and as there are no Cu-O bridges between the chains, the 1D resistivity behavior is expected. For larger hole doping however, where the magnetic interactions have changed, $\sigma(T)$ does not follow $\exp(T^{-1/2})$. Shown in the inset of Fig. 7 is also a plot of $\log_{10}\sigma(T)$ vs $1/T$ for $Ca_4Cu_5O_{10}$. The resistivity for this material more closely follows that of thermally activated conduction across a gap, $\sigma(T) \propto \exp(-\Delta/k_BT)$ with $\Delta \approx 0.08$ eV, similar in magnitude to that seen for polycrystalline $(Sr,Ca)_{14}Cu_{24}O_{41}$ under ambient pressure.[9] Thus these preliminary data suggest a crossover in the transport properties to activated behavior in the Zhang-Rice singlet regime. Significantly, we find no indication in the resistivity of charge ordering along the chains such as is seen in $(Sr,Ca)_{14}Cu_{24}O_{41}$. Further studies of the transport properties of single crystals will be required to confirm the data from polycrystalline samples and clarify the behavior.

CONCLUSIONS

We have identified and studied the simplest Cu-O chain compound with edge-sharing CuO_4 plaquettes which can be significantly doped with holes. We find the magnetic ground state to cross over from a Néel state at low hole concentrations to a short-range ordered (spin-liquid-like) ground state at high hole concentrations. We show that this is the result of hole-induced changes in the magnetic coupling, and associate the changes with the modification of superexchange paths due to the presence of Zhang-Rice singlets. The relative crystallographic simplicity, along with the strength and sign of the magnetic interactions, make this compound series an excellent model system for linking experimental and theoretical studies of the spin and charge dynamics in electronically doped low-dimensional copper oxides.

ACKNOWLEDGMENTS

We are grateful to P. Matl, J. Rijssenbeek, and Professor N. P. Ong for help in the electrical resistivity measurements. This work was partially supported by NSF (DMR-94-00362).

*Also at Institute for Solid State Physics, University of Tokyo, Roppongi, Japan.

[1] E. Dagotto and T. M. Rice, Science **271**, 618 (1996).

[2] Z. Hiroi, M. Azuma, M. Takano, and Y. Bando, J. Solid State Chem. **95**, 230 (1991).

[3] M. Azuma, Z. Hiroi, M. Takano, K. Ishida, and Y. Kitaoka, Phys. Rev. Lett. **73**, 3463 (1994).

[4] K. Ishida, Y. Kitaoka, K. Asayama, M. Azuma, Z. Hiroi, and M. Takano, J. Phys. Soc. Jpn. **63**, 3222 (1994).

[5] K. Kojima, A. Karen, G. M. Luke, B. Nachumi, W. D. Wu, Y. J. Uemura, M. Azuma, and M. Takano, Phys. Rev. Lett. **74**, 2812 (1995).

[6] M. Uehara, T. Nagata, J. Akimitsu, H. Takahashi, N. Mori, and K. Kinoshita, J. Phys. Soc. Jpn. **65**, 2764 (1996).

[7] M. Kato, H. Chizawa, Y. Koike, T. Noji, and Y. Saito, Physica C **235-240**, 1327 (1994).

[8] M. Kato, K. Shiota, and Y. Koike, Physica C **258**, 248 (1996).

[9] S. A. Carter, B. Batlogg, R. J. Cava, J. J. Krajewski, W. F. Peck, Jr., and T. M. Rice, Phys. Rev. Lett. **77**, 1378 (1996).

[10] F. C. Zhang and T. M. Rice, Phys. Rev. B **37**, 3759 (1988).

[11] T. Siegrist, R. S. Roth, C. J. Rawn, and J. J. Ritter, Chem. Mater. **2**, 192 (1990).

[12] K. K. Singh, D. E. Morris, and A. P. B. Sinha, Physica C **231**, 377 (1994).

[13] J. Karpinski, H. Schwer, E. Kopnin, R. Molinski, G. I. Meijer, and K. Conder, Physica C **282-287**, 77 (1997).

[14] P. K. Davies, E. Caignol, and T. King, J. Am. Ceram. Soc. **74**, 569 (1991).

[15] P. K. Davies, J. Solid State Chem. **95**, 365 (1991).

[16] v. K. Hestermann and R. Hoppe, Z. Anorg. Allg. Chem. **367**, 261 (1969).

[17] A recent Japanese language abstract briefly describes the magnetic susceptibilities of $(Ca,Y)_5Cu_6O_{12}$. The data are in agreement with our Fig. 3 (M. Kibune, S. Miyasaka, T. Tonogai, M. Nohara, H. Takagi, S. Adachi, and K. Tanabe (unpublished).

[18] F. Sapina, J. Rodríguez-Carvajal, M. Sanchis, R. Ibánez, A. Beltrán, and D. Beltrán, Solid State Commun. **74**, 779 (1990).

[19] A. Keren, L. P. Le, G. M. Luke, B. J. Steinlieb, W. D. Wu, Y. J. Uemura, S. Tajima, and S. Uchida, Phys. Rev. B **48**, 12 926 (1993).

[20] T. Ami, M. K. Crawford, R. L. Harlow, Z. R. Wang, D. C. Johnston, Q. Huang, and R. W. Erwin, Phys. Rev. B **51**, 5994 (1995).

[21] N. Motoyama, H. Eisaki, and S. Uchida, Phys. Rev. Lett. **76**, 3212 (1996).

[22] K. M. Kojima, Y. Fudamoto, M. Larkin, G. M. Luke, J. Merrin, B. Nachumi, Y. J. Uemura, N. Motoyama, H. Eisaki, S. Uchida, K. Yamada, Y. Endoh, S. Hosoya, B. J. Steinlieb, and G. Shirane, Phys. Rev. Lett. **78**, 1787 (1997).